Ocean Sci. Discuss., 9, 2375–2401, 2012
www.ocean-sci-discuss.net/9/2375/2012/
doi:10.5194/osd-9-2375-2012

Ocean Science Discussions

Sea level variability in the Arctic Ocean observed by satellite altimetry

P. Prandi[1], M. Ablain[1], A. Cazenave[2], and N. Picot[3]

[1]CLS, Space Oceanography Division, Ramonville St-Agne, France
[2]LEGOS, CNRS, Toulouse, France
[3]Centre Spatial de Toulouse, CNES, Toulouse, France

Received: 1 June 2012 – Accepted: 18 June 2012 – Published: 19 July 2012

Correspondence to: P. Prandi (pprandi@cls.fr)

Published by Copernicus Publications on behalf of the European Geosciences Union.

Abstract

We investigate sea level variability in the Arctic Ocean from observations. Variability estimates are derived both at the basin scale and on smaller local spatial scales. The periods of the signals studied vary from high frequency (intra-annual) to long term trends. We also investigate the mechanisms responsible for the observed variability. Different data types are used, the main one being a recent reprocessing of satellite altimetry data in the Arctic Ocean.

Satellite altimetry data is compared to tide gauges measurements, steric sea level derived from temperature and salinity fields and GRACE ocean mass estimates. We establish a consistent regional sea level budget over the GRACE availability era (2003–2009) showing that the sea level drop observed by altimetry over this period is driven by ocean mass loss rather than steric effects. The comparison of altimetry and tide gauges time series show that the two techniques are in good agreement regarding sea level trends. Coastal areas of high variability in the altimetry record are also consistent with tide gauges records. An EOF analysis of September mean altimetry fields allows identifying two regions of wind driven variability in the Arctic Ocean: the Beaufort Gyre region and the coastal European and Russian Arctic. Such patterns are related to atmospheric regimes through the Arctic Oscillation and Dipole Anomaly.

1 Introduction

Various parts of the Arctic climate system are undergoing changes, among them the Arctic Ocean. Certainly the most visible and most studied part of these changes is the decline of sea-ice extent (Stroeve et al., 2012), but many other can affect the Arctic Ocean: changes in ocean circulation, in freshwater content (Rabe et al., 2011; McPhee et al., 2009), in sea-ice volume (Kwok et al., 2009). Moreover, the rapid mass loss of the Greenland Ice Sheet (GIS) (Velicogna, 2009) may affect the surrounding ocean as well as have global impacts. All these effects can impact sea level, a natural integrator

OSD
9, 2375–2401, 2012

of various climatic components which is, at a global scale, an important indicator of climate change (Cazenave and Llovel, 2010; Bindoff et al., 2007). In the Arctic Ocean sea level studies mainly rely on long records by tide gauge stations (Proshutinsky et al., 2001, 2004) or outputs from models (Proshutinsky et al., 2007). For example Proshutinsky et al. (2001) found a sea level rise of 1.85 $mm\,yr^{-1}$ in the Russian Arctic over 1954–1989 and Proshutinsky et al. (2007) used model runs from the AOMIP project to determine the characteristics of sea level variability in the Arctic. Proshutinsky and Johnson (1997) identified two wind regimes driving oceanic circulation and affecting sea level in the Arctic Ocean, recent updates on the wind regime were given by Proshutinsky et al. (2011, 2009a). One of the first use of satellite altimetry to estimate sea surface height in the Arctic Ocean was made by Peacock and Laxon (2004) and their technique was used by Scharroo et al. (2006) who estimated a sea level drop from ERS-2 data over 1995–2003. Investigations were also conducted on the steric part by Seigismund et al. (2007) but limited to the Nordic Seas. Recently efforts were made to use satellite altimetry data in the Arctic Ocean to study long-term sea level variability. Prandi et al. (2012) used a dedicated regional processing to build a dataset suitable for studying sea level variability in the Arctic Ocean over the 1993–2009 period with an effort to use reference missions to provide a stable baseline. Henry et al. (2012) analyzed sea level estimates from different techniques in the Nordic Seas with a long term perspective and Giles et al. (2012) derived freshwater content change from satellite altimetry measurements and linked them to the wind induced spin-up of the Beaufort gyre.

In this study we investigate sea level variability in the Arctic Ocean from observations over the 1993–2009 period. Different periods from high-frequency signals to long term trends are considered, both at the basin wide scale and at smaller spatial scales. Sea level data derived from different techniques are used and compared. First we discuss the observation capabilities of the different techniques used in the Arctic Ocean: satellite altimetry, tide gauges, temperature and salinity data and GRACE ocean mass data. We perform a regional comparison of altimetry based sea level to ocean mass and steric sea level estimations to look at the regional sea level budget. Local comparisons are performed at tide gauges stations for the variability levels and for long term drift. Patterns of altimetry SLA in the Arctic Ocean are derived from an EOF analysis and compared to modeled wind forcing response.

2 Arctic Ocean observation capabilities

2.1 Satellite altimetry

In this study we use the dataset produced by Prandi et al. (2012). The dataset consists of 887 weekly grids of sea level anomaly, at 1/8° resolution, covering all latitudes between 50° N and 82° N and from January 1993 to December 2009. The processing of this dataset was dedicated to the Arctic Ocean. The data used to map sea level anomaly in the Arctic Ocean come from ERS-1, ERS-2, GFO and Envisat missions north of 66° N but all missions were linked to the baseline provided by Topex/Poseidon, Jason-1 and Jason-2 data to ensure the stability of the dataset over time. Only the ice-free ocean is observed by satellite altimetry, as a consequence some areas of the Arctic Ocean are only sampled by the dataset in summer (Prandi et al., 2012), the ocean data coverage is presented on Fig. 1. The altimetry data processing used is subject to errors which were evaluated and resulted in a 1.3 mm yr^{-1} uncertainty (with 90 % confidence) applied to the regional trend derived over the whole period. For this study, to ensure consistency with other datasets, we used monthly means derived from the weekly grids.

2.2 Tide gauges data

Tide gauges stations provide independent relative sea level measurements that can be usefully compared to satellite altimetry data. In this study we use monthly tide gauge time series obtained from the Permanent Service for Mean Sea Level (PSMSL, Woodworth and Player, 2003) database. We selected all stations containing data over the

OSD
9, 2375–2401, 2012

1993–2009 period and with latitudes greater than 60° N. Such selection criteria are applied to match the time-space domain covered by the satellite altimetry dataset. We therefore use a subset of 46 stations whose positions are presented on Fig. 1. Although the distribution of the stations along the coasts of the Arctic basin is good with stations all around the Arctic Ocean some areas like the coasts of Norway are oversampled and the American and Canadian coasts have only four stations. The temporal data coverage is also very uneven, many time series have large gaps, and this is especially true for stations in Siberia and in the Canadian Arctic. The tide gauges stations positions, as well as the completeness of the time series over the satellite altimetry time span are presented on Fig. 1. Tide gauges stations in the area are subject to important vertical land motion due to the GIA effect. This effect has to be removed to allow comparison with satellite altimetry data, the time series are corrected for the GIA effect using ICE5G_VM4 model (Peltier, 2004, 2009). Other GIA models are available such as ICE3G and ICE5G_VM2 and differences between the models can be large as reported by Henry et al. (2012). The ICE5G_VM4 model is selected after comparison with satellite altimetry data and other works who suggest it performs best (Bouin and Wöppelmann, 2010). The stations might be subject to other vertical land motion than the GIA, unfortunately with no GPS data available these motions cannot be corrected. To be consistent with satellite altimetry, tide gauges time series are also corrected for the inverted barometer effect using monthly sea level pressure fields from the NCEP/NCAR reanalysis (Kalnay et al., 1996).

2.3 Temperature and salinity data

To get an estimate of the steric part of sea level variability in the Arctic Ocean we use the EN3 dataset (Ingleby and Huddleston, 2007). The temperature and salinity profiles used to create EN3's monthly three dimensional grids mainly come from WOD05 (Levitus et al., 2005), GTSPP (Sun and et al., 2010) and Argo (http://www.argo.ucsd.edu) databases. In the Arctic data from the Arctic Synoptic Basin-wide Observations (ASBO, http://www.noc.soton.ac.uk/ooc/ASBO/index.php) project are included enhancing the

OSD
9, 2375–2401, 2012

data coverage in the region. Even with the addition of the ASBO data, the sampling of the ocean remains low with a mean of 250 profiles available for each month north of 66° but with a large annual signal in the number of profiles. The sampling is good in the Greenland, Iceland, Norway (GIN) Sea and in the Beaufort Sea. The data coverage is very low in the Russian Arctic. The number of profiles used to calculate the EN3 grids and the corresponding mean depth over time is presented on Fig. 2. To evaluate steric sea level, we integrate the density deviation with respect to a reference temperature and salinity over the whole water column, thus obtaining a series of monthly steric sea level height grids at one degree resolution. On a global scale, the deployment of ARGO profilers has greatly improved the T/S sampling of the ocean, however very few ARGO floats are available in the Arctic Ocean and the sampling does not really improve in the latest part of the period.

2.4 GRACE ocean mass data

The GRACE mission was launched in 2002 and provides a way to evaluate mass changes of the ocean affecting sea level. In this study we use GRACE fields computed by Chambers (2006), we used the CSR version of the release 04 of the data. The period common to altimetry and GRACE data is reduced to less than 8 yr from 2002 to 2009. In general, continental signals are larger than oceanic signals and can leak over ocean. In the region, the large GIS mass loss represents a very important GRACE signal that can induce such leakage of the continental signal over the ocean. To prevent pollution of the ocean signal the fields we use include a correction to minimize continental leakage, but this effect might not be completely removed. GRACE data is also sensitive to the GIA and the effect averaged over the global ocean is still uncertain ranging from $-1\,\mathrm{mm\,yr^{-1}}$ (Paulson et al., 2007) to $-2\,\mathrm{mm\,yr^{-1}}$ (Peltier, 2009), at high latitudes this effect is likely more important than the global average. The GRACE grids used in this study are corrected for the GIA using the model by Paulson et al. (2007).

OSD
9, 2375–2401, 2012

3 Description of the observed variability

3.1 Regional variability and trends

The SLA time series over the 66° N to 82° N region is displayed on Fig. 3 (red), the variability observed is large with a mean SLA standard deviation of 2.0 cm after removing the trend (the standard deviation is 0.2 cm for the global MSL time series). Over the whole period the SLA shows a rising trend of 3.6 mm yr^{-1}. In their paper presenting the data Prandi et al. (2012) make an estimation of the uncertainty affecting the trend estimation over the 1993–2009 period. They find that due to the measurement and processing errors only, the uncertainty on the trend amounts to 1.3 mm yr^{-1} with 90 % confidence. This uncertainty value does not account for the impact of temporally correlated variability on the trend value estimate over a given period. Such effect is low on the global average sea level as the inter-annual variability levels are low (Ablain et al., 2009) but can have a significant impact when considering regional averages. In order to evaluate the trend sensitivity to the study period, we estimate Arctic regional sea level trends over 10 yr running windows from 1993–2002 to 2000–2009. The results are presented on Fig. 3 in blue. Trends were estimated from monthly mean time series and after removing the seasonal signal. The large variability of SLA leads to 10 yr trends ranging from 1.6 to 6.2 mm yr^{-1}. There appears to be a shift in sea level trends in the second part of the period: after 2003, the 10-year trend shows an important reduction. Given the uncertainty level of 1.3 mm yr^{-1} previously presented all 10 yr periods show a significantly positive trend.

The total sea level rise measured by satellite altimetry is the sum of steric and mass components. The steric part can be evaluated from temperature and salinity data. For the last 7 yr of the altimetry record (2003–2009), GRACE ocean mass data is available and provides a way to evaluate the mass component. The availability of the three records gives the opportunity to investigate the Arctic regional sea level rise budget. We compare satellite altimetry, steric sea level derived from EN3 dataset and ocean mass from GRACE over the oceanic domain bound between 66° N and 82° N. The analysis

OSD
9, 2375–2401, 2012

is performed over the 2003–2009 period which is common to the three datasets used. Monthly sea level time series are computed from altimetry, GRACE and EN3 datasets representing the total, mass and steric components of sea level change, respectively. Steric and mass parts are summed up and compared to the altimetry record. Figure 4 presents the time series obtained from altimetry and from the sum of mass and steric components, averaged over all ocean grid points with latitudes between 66° N and 82° N. A very good agreement is found between the two records, the correlation coefficient is $r = 0.75$ and the standard deviation of the differences is 2 cm. Regarding the long-term trend, the satellite altimetry record displays a sea level drop at a rate of $-4.3\,\mathrm{mm\,yr^{-1}}$ compared to $-4.8\,\mathrm{mm\,yr^{-1}}$ for the sum of mass and steric contributions. Separating the mass and steric components of sea level change, it appears that both the steric and mass parts contribute to the drop observed over the period with negative trend values of $-0.5\,\mathrm{mm\,yr^{-1}}$ and $-4.3\,\mathrm{mm\,yr^{-1}}$ over 2009–2009, respectively. A decrease of the Arctic Ocean mass has been previously reported from comparisons between GRACE data and records of bottom pressure near the North Pole (Morison et al., 2007). Here we find that the negative SL trend observed by altimetry over 2009–2009 is dominated by the Arctic Ocean mass loss rather than steric change.

Considering the annual cycle, amplitudes are 7 and 4.4 cm for altimetry and the sum of ocean mass and steric sea level. The uneven coverage of the Arctic Ocean by the altimetry dataset can be responsible for the differences: as large parts of the Arctic Ocean interior are not observed all year long the winter months sampling is biased towards the Nordic Seas. If we consider mass and steric grid points only if there is a valid satellite record at the corresponding space and time (therefore applying the same spatial bias to all datasets) the annual cycle's amplitudes show a better agreement with 7 and 6 cm for the altimetry and sum of mass and steric components, respectively. The annual cycles for altimetry, steric sea level, GRACE ocean mass and the sum of ocean mass and steric are represented on Fig. 5. The maximum is reached in January for the altimetry and in October for the sum of steric and mass parts, the minimum occurs in April for both estimates. It appears that the annual cycle is mainly driven by changes in

OSD

9, 2375–2401, 2012

Sea level variability in the Arctic Ocean observed by satellite altimetry

P. Prandi et al.

steric sea level (amplitude 4.5 cm) rather than ocean mass changes (amplitude 2.3 cm). It is interesting to note that the shape of the annual cycle derived from altimetry shows a local maximum reached in July consistent previous estimates from tide gauges data (Proshutinsky et al., 2007), however the sum of ocean mass and steric parts does not show the same feature.

3.2 Local variability and trends

To estimate the spatial distribution of the observed temporal variability we calculate the map of monthly SLA RMS. The result is presented on Fig. 6. It appears that high variability areas are concentrated along the coastlines. The area experiencing the most important variability is the Canadian Arctic Archipelago but the errors are likely high in this area mainly due to tidal prediction in a complex geometry and bathymetry and to other problems affecting altimetry in coastal areas. The East Siberian Sea is another area where sea level variability is important with respect to other parts of the basin. High variability areas are located in shallow water regions and this could indicate an error of the altimetry processing. In order to validate the altimetry observations we perform a comparison to tide gauge stations. For each tide gauge we evaluate the correlation coefficient with satellite altimetry grid points within 200 km of the tide gauge position. The altimetric time series is extracted where the maximum of correlation with the tide gauge time series is found (Valladeau et al., 2012). The position of the tide gauges stations, as well as the correlations with altimetry are presented on Fig. 7. 7 stations fail to show correlations statistically different from 0 at the 1 % level and are excluded from further analysis; those stations are circled in red on Figs. 6–8. Excluding these stations from the comparison, the mean correlation coefficient is 0.6 with values ranging from 0.3 at Ny-Alesund (Greenland Sea) to 0.77 at Izvestia (Kara Sea). The tide gauge sea level RMS levels are overlaid on Fig. 6. The comparison shows that altimetry SLA time series generally display lower variability than tide gauges time series. For the mean of 39 stations, collocated SLA RMS values are 9.2 cm and 15.3 cm for altimetry and tide gauges, respectively. The local maximum for SLA RMS in the East Siberian

OSD
9, 2375–2401, 2012

Sea seen in the altimetry data is also seen by the tide gauges situated in this area, indicating that the high variability in this area likely results from a physical signal rather than an altimetry error.

The variability estimated by the RMS is dominated by short term signals, in order to evaluate long-term variability we estimate SLA trends over the whole 1993–2009 period covered by the satellite altimetry dataset, the map of sea level trends is presented on Fig. 8. There is a large positive signal around the southern tip of Greenland that was already observed in global datasets. Regarding long term trends, the agreement between altimetry and tide gauges is good; the tide gauges trends are superimposed to the map of altimetry trends on Fig. 8. Averaging the 39 stations, the collocated altimetry trend is 5.2 $mm\,yr^{-1}$, larger than the 4.3 $mm\,yr^{-1}$ obtained from tide gauge data. The mean drift is 0.9 $mm\,yr^{-1}$, a value smaller than the uncertainty affecting altimetry trends determination. At some stations the altimetry and tide gauges trends are very different, the largest difference is found at station Shalaurova (East Siberian Sea) with a 9 $mm\,yr^{-1}$ drift due to gaps in both time series leading to a trend evaluation based on very different periods. When both techniques are strictly matched over time (i.e. using a satellite measurement only if a tide gauge measurement is available at the same time and respectively) the drift is reduced to 0.2 $mm\,yr^{-1}$. Both mean drift values are lower than the uncertainty affecting the altimetry trend estimation over the whole period (1.3 $mm\,yr^{-1}$).

In the Arctic interior, the largest trend signal is found in the Beaufort Gyre where sea level rise rates can reach values greater than 15 $mm\,yr^{-1}$. The observed sea level rise in the Beaufort Gyre is consistent with results previously reported using a different processing of satellite altimetry data (Giles et al., 2012) and estimates of freshwater change in the basin Proshutinsky et al. (2009b) indicating a freshwater accumulation in the Beaufort Gyre for recent years. We perform an Empirical Orthogonal Functions (EOF) analysis of September SLA fields in the region bound by 66° N to 82° N latitudes and 190° E to 270° E longitudes. The second mode of altimetry SLA explains 21 % of the signal variance and is presented on Fig. 9. This mode has a spatial pattern

OSD
9, 2375–2401, 2012

corresponding to the Beaufort Gyre circulation. The associated principal component is correlated ($r = 0.66$) to the Dipole Anomaly (Wu et al., 2006) suggesting a wind-driven effect. Observation of such SLA signature of a wind-driven spin up of the cyclonic circulation in the altimetry dataset is a confirmation of a previous study by Giles et al. (2012).

3.3 Wind-driven variability over the European Arctic shelf

Both the satellite and tide gauge data display an area of high sea level variability along the coasts of the Russian Arctic, the maximum of altimetry SLA RMS is reached in the East Siberian Sea, confirmed by tide gauge records available in the sector (see Fig. 6). The areas of high sea level variability look coherent with the bathymetry which could indicate errors in the altimetry processing although agreement with tide gauges points toward a physical process. In order to characterize the observed SLA variability, we compute the EOF of the satellite dataset. The sampling of the ocean in the Arctic interior is heavily biased towards the summer season when the ice-covered area reaches its minimum. In order to get maximum coverage of the ocean we therefore analyze September mean SLA fields (results are similar when considering JAS means). The first mode of September SLA is represented on Fig. 10 (left panel), it explains 29 % of the total SLA variance. This mode displays a pattern similar to the one observed in the SLA RMS map with the variability concentrated along the European and Russian Arctic coasts indicating that part of this signal has an inter-annual origin. The principal component associated with the first mode is strongly correlated ($r = 0.78$, statistically different from 0 at the 1 % level) with the September Arctic Oscillation Index (AOI, Thompson and Wallace, 1998). The principal component and the AOI show a very similar behavior both on year-to-year and longer timescales (see Fig. 10, bottom panel). Such correlation with an atmospheric based index, along with the agreement with tide gauge variability, discards an error of the altimetry processing as the principal driver for the observed high variability in the region. The correlation to the AOI, a SLP based indicator, likely indicates a response of the SLA to atmospheric forcing.

OSD
9, 2375–2401, 2012

In the altimetry processing, atmospheric effects on the SLA are accounted for by the dynamic atmospheric correction which is the sum of two terms. The first corresponds to the static inverted barometer (IB) effect and the second to the dynamic response of the ocean to wind and pressure. The IB, very closely related to the AO, has a long scale spatial signature (not shown) which is very different from the pattern of the first SLA EOF. The dynamic response of SLA to wind and pressure forcing is estimated by the Mog2d model (Carrère and Lyard, 2003). The outputs of the model are filtered to remove all signals with periods greater than 20 days corresponding to the temporal resolution achievable by the 10 days cycles of T/P and Jason missions, the resulting high frequency signal is then removed from altimetry data. We perform an EOF analysis on September mean Mog2d fields after applying a Lanczos filter to remove signals with periods smaller than 20 days. The resulting fields represent the low-frequency part of the SLA response to wind forcing which is not removed from altimetry data as it represents a physical process of the ocean that the altimetry is able to resolve. The first EOF explains 45 % of the total variance of Mog2d September mean fields and is presented on Fig. 10 (right panel), it displays a very similar spatial pattern of variability than the first SLA EOF with the largest signal found along the European and Russian Arctic coasts and in the East Siberian Sea. The principal component is strongly correlated to the altimetry SLA principal component ($r = 0.83$) and to the AOI ($r = 0.76$). The agreement between the altimetry observations and the low frequencies of Mog2d model shows that inter-annual September SLA variability in the Russian sector of the Arctic Ocean is dominated by the dynamic response of the ocean to atmospheric forcing. This response is thus related to the Arctic Oscillation which affects the atmospheric pressure patterns and the wind regime. A previous study based on the analysis of ocean models demonstrated an agreement between the first principal component of the modeled SLA in the Arctic and the AO on decadal timescales (Proshutinsky et al., 2007). Here we demonstrate that on shorter time scales, and over a shorter analysis period, the satellite altimetry record is observing a dominant wind-driven, AO related, variability in the coastal European and Russian Arctic.

OSD
9, 2375–2401, 2012

4 Summary and conclusions

In this study we used different type of data to describe and investigate sea level variability in the Arctic Ocean over the 1993–2009 period. We demonstrate that the regional sea level time series high variability has an important impact on 10 yr trends but that over all the 10 yr windows available the sea level trends remained constantly positive given the 1.3 mm yr^{-1} uncertainty level. For the last part of the record (2003–2009) the combination of GRACE ocean mass data and steric sea level estimates allows to derive a consistent regional sea level budget for the Arctic Ocean. Over this short period, the satellite record exhibits a negative sea level rise trend which is mainly explained by ocean mass loss in the region. We establish that the high regional variability is unevenly distributed in the Arctic Ocean, the coastal areas of the Russian Arctic exhibit the largest variability levels. Tide gauge data available in the basin generally show higher levels of variability than altimetry but the spatial distribution of tide gauge RMS is in agreement with altimetry suggesting that the altimetry derived variability levels result from a physical signal rather than errors. Regarding the sea level trends, the agreement is good although some stations show large differences; in some cases the tide gauge data can be questioned. In the East Siberian Sea, where the SLA variability is high in both the altimetry and tide gauges records, we showed that first mode of September mean variability is closely correlated to the Arctic Oscillation and results from low frequency wind-driven SLA changes as a consequence of the modification of the atmospheric circulation. A similar process is likely occurring in the Beaufort Gyre region, in relation with the Arctic Dipole Anomaly. A continuous monitoring of the Arctic Ocean is still necessary as processes crucial for climate might be detected through sea level rise. The recent launch of CryoSat-2 mission and the future launch of SARAL/AltiKa and Sentinel-3 missions will certainly permit such monitoring from the altimetry side.

Acknowledgements. P. Prandi is funded by a PhD grant from CNES and CLS. This work contributes to the European FP7 MONARCH-A project.

OSD
9, 2375–2401, 2012

Sea level variability in the Arctic Ocean observed by satellite altimetry

P. Prandi et al.

References

Ablain, M., Cazenave, A., Valladeau, G., and Guinehut, S.: A new assessment of the error budget of global mean sea level rate estimated by satellite altimetry over 1993–2008, Ocean Sci., 5, 193–201, doi:10.5194/os-5-193-2009, 2009. 2381

Bindoff, N., Willebrand, J., Artale, V., Cazenave, A., Gregory, J. M., Gulev, S., Hanawa, H., Le Quéré, C., Levitus, S., Nojiri, Y., Shum, C. K., Talley, L., and Unnikrishnan, A.: Observations: oceanic climate change and sea level, in: Climate change 2007: The physical Science Basis. Contribution of Working Group I to the Fourth Assessment Report of the Intergovernmental Panel on Climate Change, edited by: Solomon, S., Qin, D., Manning, M., Chen, Z., Marquis, M., Averyt, K. B., Tignor, M., and Miller, H. L., Cambridge University Press, UK and New York, USA, 385–432, 2007. 2377

Bouin, M. N. and Wöppelmann, G.: Land motion estimates from GPS at tide gauges: a geophysical evaluation, Geophys. J. Int., 180, 193–209, 2010. 2379

Carrère, L. and Lyard, F.: Modeling the barotropic response of the global ocean to atmospheric wind and pressure forcing, comparison with observations, Geophys. Res. Lett., 30, 1275, doi:10.1029/2002GL016473, 2003. 2386

Cazenave, A. and Llovel, W.: Contemporary sea level rise, Annu. Rev. Mar. Sci., 2, 145–173, doi:10.1146/annurev-marine-120308-081105, 2010. 2377

Chambers, D.: Evaluation of new GRACE time-variable gravity data over the ocean, Geophys. Res. Lett., 33, L17603, 2006. 2380

Giles, K. A., Laxon, S. W., Ridout, A. L., Wingham, D. J., and Bacon, S.: Western Arctic Ocean freshwater storage increased by wind-driven spin-up of the Beaufort Gyre, Nat. Geosci., 5, 194–197, doi:10.1038/NGEO1379, 2012. 2377, 2384, 2385

Henry, O., Prandi, P., Llovel, W., Cazenave, A., Jevrejeva, S., Stammer, D., Meyssignac, B., and Koldunov, N.: Tide gauge based Sea level variations since 1950 along the Norwegian and Russian coasts of the Arctic Ocean; contribution of the steric component, J. Geophys. Res., 117, C06023, 2012. 2377, 2379

Ingleby, B. and Huddleston, M.: Quality control of ocean temperature and salinity profiles – historical and real-time data, J. Marine Syst., 65, 158–175, doi:10.1016/j.jmarsys.2005.11.019, 2007. 2379

Kalnay, E., Kanamitsu, M., Kistler, R., Collins, W., Deaven, D., Gandin, L., Iredell, M., Saha, S., White, G., Woollen, J., Zhu, Y., Leetmaa, A., Reynolds, B., Chelliah, M., Ebisuzaki, W.,

OSD
9, 2375–2401, 2012

Title Page
Abstract | Introduction
Conclusions | References
Tables | Figures
◂| |▸
◂ ▸
Back | Close
Full Screen / Esc
Printer-friendly Version
Interactive Discussion

Higgins, W., Janowiak, J., Mo, K. C., Ropelewski, C., Wang, J., Jenne, R., and Joseph, D.: The NCEP/NCAR 40-year reanalysis project, B. Am. Meteorol. Soc., 77, 437–472, 1996. 2379

Kwok, R., Cunningham, G. F., Wensnahan, M., Rigor, I., Zwally, H. J., and Yi, D.: Thinning and volume loss of the Arctic Ocean sea ice cover: 2003–2008, J. Geophys. Res., 114, C07005, doi:10.1029/2009JC005312, 2009. 2376

Levitus, S., Antonov, J., and Boyer, T.: Warming of the world ocean, 1955–2003, Geophys. Res. Lett., 32, L02604, doi:10.1029/2004GL021592, 2005. 2379

McPhee, M. G., Proshutinsky, A., Morison, J. H., Steele, M., and Alkire, M. B.: Rapid change in freshwater content of the Arctic Ocean, Geophys. Res. Lett., 36, L10602, doi:10.1029/2009GL037525, 2009. 2376

Morison, J., Wahr, J., Kwok, R., and Peralta-Ferriz, C.: Recent trends in Arctic Ocean mass distribution revealed by GRACE, Geophys. Res. Lett., 34, L07602, doi:10.1029/2006GL029016, 2007. 2382

Paulson, A., Zhong, S., and Wahr, J.: Limitations on the inversion for mantle viscosity from postglacial rebound, Geophys. J. Int., 168, 1195–1209, doi:10.1111/j.1365-246X.2006.03222.x, 2007. 2380

Peacock, N. R. and Laxon, S. W.: Sea surface height determination in the Arctic Ocean from ERS altimetry, J. Geophys. Res., 109, C07001, doi:10.1029/2001JC001026, 2004. 2377

Peltier, W. R.: Global glacial isostasy and the surface of the ice-age Earth: the ICE-5G (VM2) model and GRACE, Annu. Rev. Earth Pl. Sc., 32, 111–149, 2004. 2379

Peltier, W. R.: Closure of the budget of global sea level rise over the GRACE era: the importance and magnitudes of the required corrections for global isostatic adjustment, Quaternary Sci. Rev., 28, 1658–1674, 2009. 2379, 2380

Prandi, P., Ablain, M., Cazenave, A., and Picot, N.: A new estimation of mean sea level in the Arctic Ocean from satellite altimetry, Mar. Geod., accepted, 2012. 2377, 2378, 2381

Proshutinsky, A. and Johnson, M. A.: Two circulation regimes of the wind-driven Arctic Ocean, J. Geophys. Res., 102, 12493–12514, doi:10.1029/97JC00738, 1997. 2377

Proshutinsky, A., Pavlov, V., and Bourke, R. H.: Sea level rise in the Arctic Ocean, Geophys. Res. Lett., 28, 2237, doi:10.1029/2000GL012760, 2001. 2377

Proshutinsky, A., Ashik, I., Dvorkin, E. N., Hakkinen, S., Krishfield, R., and Peltier, W. R.: Secular sea level change in the Russian sector of the Arctic Ocean, J. Geophys. Res., 109, C03042, doi:10.1029/2003JC002007, 2004. 2377

Proshutinsky, A., Ashik, I., Häkkinen, S., Hunke, E., Krishfield, R., Maltrud, M., Maslowski, W., and Zhang, J.: Sea level variability in the Arctic Ocean from AOMIP models, J. Geophys. Res., 112, C04S08, doi:10.1029/2006JC003916, 2007. 2377, 2383, 2386

Proshutinsky, A., Krishfield, R., Steele, M., Polyakov, I., Ashik, I., McPhee, M., Morison, J., Timmermans, M.-L., Toole, J., Sokolov, V., Frolov, I., Carmack, E., McLaughlin, F., Shimada, K., Woodgate, R., and Weingartner, T.: Ocean, in: State of the Climate in 2008, B. Am. Meteorol. Soc., 90, 99–102, 2009a. 2377

Proshutinsky, A., Krishfield, R., Timmermans, M.-L., Toole, J., Carmack, E., McLaughlin, F., Williams, W. J., Zimmermann, S., Itoh, M., and Shimada, K.: Beaufort Gyre freshwater reservoir: state and variability from observations, J. Geophys. Res., 114, C00A10, doi:10.1029/2008JC005104, 2009b. 2384

Proshutinsky, A., Timmermans, M. L., Ashik, I., Beszczynska-Moeller, A., Carmack, E., Frolov, I., Krishfield, R., McLaughlin, F., Morison, J., Polyakov, I., Shimada, K., Sokolov, V., Steele, M., Toole, J., and Woodgate, R.: The Arctic (Ocean), in: State of the Climate in 2010, B. Am. Meteorol. Soc., 92, S145–S148, 2011. 2377

Rabe, B., Karcher, M., Schauer, U., Toole, J. M., Krishfield, R., Pisarev, S., Kauker, F., Gerdes, R., and Kikuchi, T.: An assessment of Arctic Ocean freshwater content changes from the 1990s to the 2006–2008 period, Deep-Sea Res. Pt. I, 58, 173–185, doi:10.1016/j.dsr.2010.12.002, 2011. 2376

Scharroo, R., Ridout, A. L., and Laxon, S. W., Arctic sea level change from satellite altimetry, Eos Trans. AGU, 87(36), Jt. Assem. Suppl., Abstract G21A-02, 2006. 2377

Seigismund, F., Johannessen, J., Drange, H., Mork, K. A., and Korablev, A.: Steric height variability in the nordic seas, J. Geophys. Res., 112, C12010, doi:10.1029/2007JC004221, 2007. 2377

Stroeve, J., Serreze, M., Holland, M., Kay, J., Malanik, J., and Barrett, A.: The Arctic's rapidly shrinking sea ice cover: a research synthesis, Climatic Change, 110, 1005–1027, doi:10.1007/s10584-011-0101-1, 2012. 2376

Sun, C., Thresher, A., Keeley, R., Hall, N., Hamilton, M., Chinn, P., Tran, A., Goni, G., Petit de la Villeon, L., Carval, T., Cowen, L., Manzella, G., Gopalakrishna, V., Guerrero, R., Reseghetti, F., Kanno, Y., Klein, B., Rickards, L., Baldoni, A., Lin, S., Ji, F., Nagaya, Y.: The data management system for the global temperature and salinity profile programme, in: Proceedings of OceanObs.09: sustained ocean observations and information for society, vol. 2, edited by: Hall, J., Harrison, D., and Stammer, D., WPP-306, ESA Publication, Venice, Italy, doi:10.5270/OceanObs09.cwp.86, 2010. 2379

Thompson, D. W. J. and Wallace, J. M.: The Arctic oscillation signature in the wintertime geopotential height and temperature fields, Geophys. Res. Lett., 25, 1297–1300, 1998. 2385

Valladeau, G., Legeais, J.-F., Ablain, M., Guinehut, S., and Picot, N.: Comparing altimetry with tide gauges and Argo profiling floats for data quality assessment and mean sea level studies, Mar. Geod., accepted, 2012. 2383

Velicogna, I.: Increasing rates of ice mass loss from the Greenland and Antarctic ice sheets revealed by GRACE, Geophys. Res. Lett., 36, L19503, doi:10.1029/2009GL040222, 2009. 2376

Woodworth, P. and Player, R.: The permanent service for mean sea level: an update to the 21st century, J. Coastal Res., 19, 287–295, permanent Service for Mean Sea Level (PSMSL), 2012, Tide Gauge Data, available at: http://www.psmsl.org/data/obtaining/, last access: November 2011, 2003. 2378

Wu, B., Wang, J., and Walsh, J. E.: Dipole anomaly in the winter arctic atmosphere and its association with sea ice motion, J. Climate, 19, 210–225, 2006. 2385

OSD

9, 2375–2401, 2012

Sea level variability in the Arctic Ocean observed by satellite altimetry

P. Prandi et al.

Title Page
Abstract | Introduction
Conclusions | References
Tables | Figures
◀| |▶
◀ ▶
Back | Close
Full Screen / Esc
Printer-friendly Version
Interactive Discussion

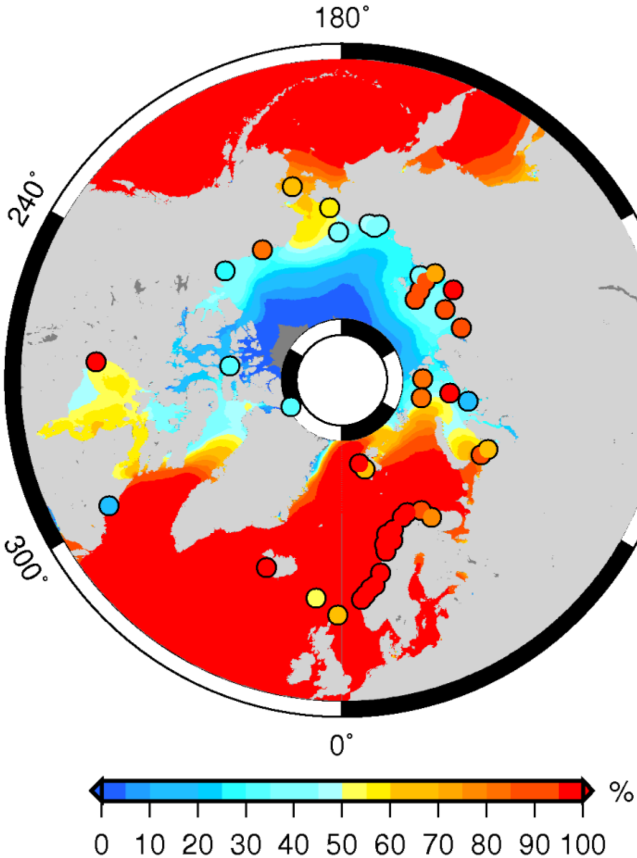

Fig. 1. Data coverage in the Arctic Ocean (percentage of monthly grids with a valid measurement) for satellite altimetry (background) and tide gauges records (black circles).

OSD
9, 2375–2401, 2012

Sea level variability in the Arctic Ocean observed by satellite altimetry

P. Prandi et al.

Title Page
Abstract | Introduction
Conclusions | References
Tables | Figures
◀| |▶
◀ ▶
Back | Close
Full Screen / Esc
Printer-friendly Version
Interactive Discussion

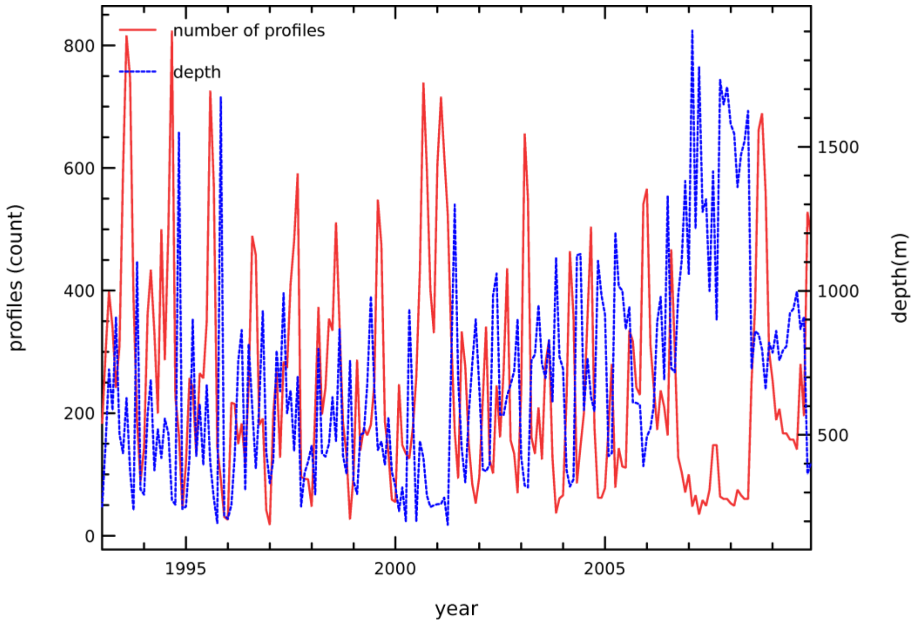

Fig. 2. Time series of the number (red) and depth (blue) of the T/S profiles en EN3 analysis.

OSD
9, 2375–2401, 2012

Sea level variability in the Arctic Ocean observed by satellite altimetry

P. Prandi et al.

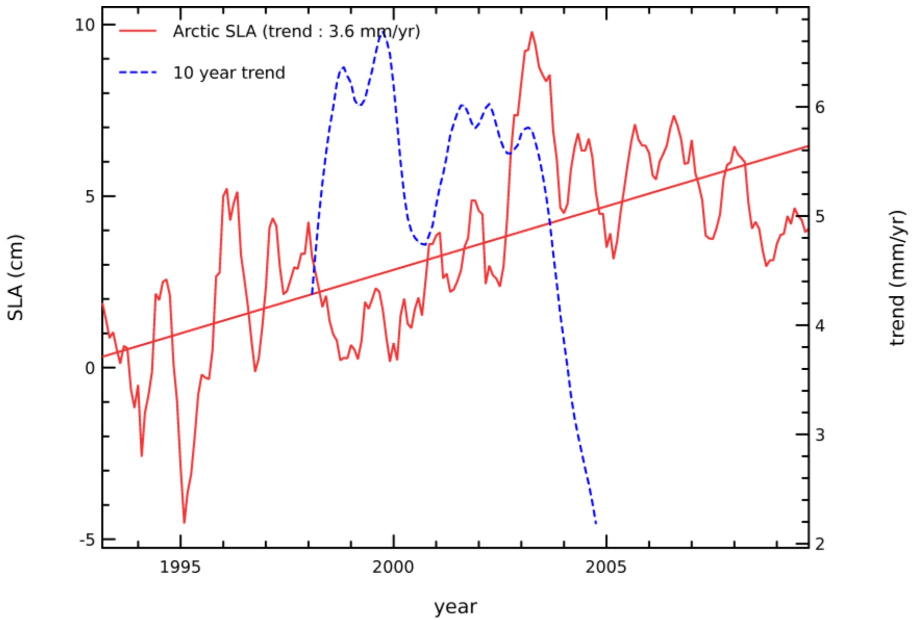

Fig. 3. Time series of satellite altimetry SLA in the Arctic Ocean (red, in cm) and 10 yr trends (blue, in $mm\,yr^{-1}$).

OSD
9, 2375–2401, 2012

Sea level variability in the Arctic Ocean observed by satellite altimetry

P. Prandi et al.

Title Page
Abstract | Introduction
Conclusions | References
Tables | Figures
◀| |▶
◀ ▶
Back | Close
Full Screen / Esc
Printer-friendly Version
Interactive Discussion

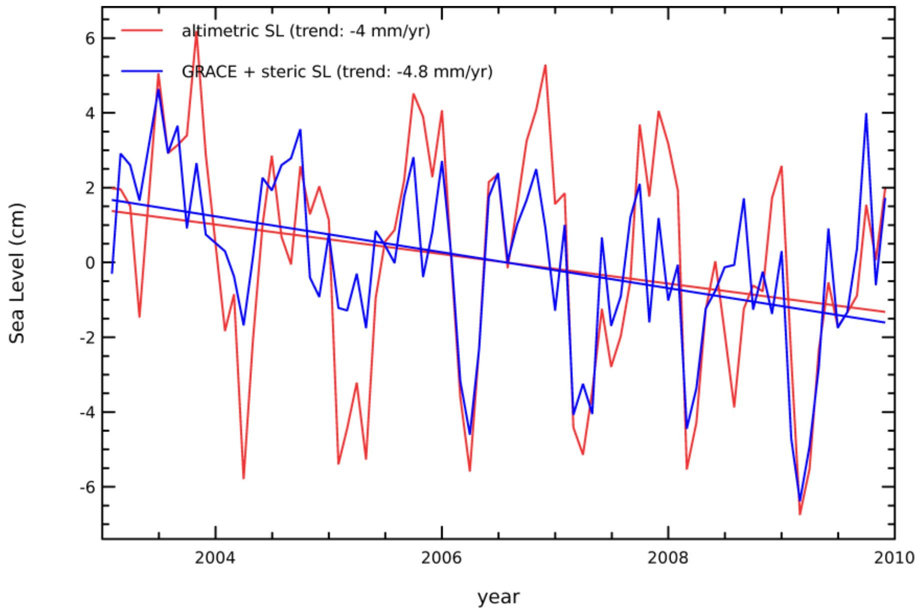

Fig. 4. Time series of satellite altimetry SLA (red) in the Arctic Ocean and of the sum of mass and steric components (blue).

OSD
9, 2375–2401, 2012

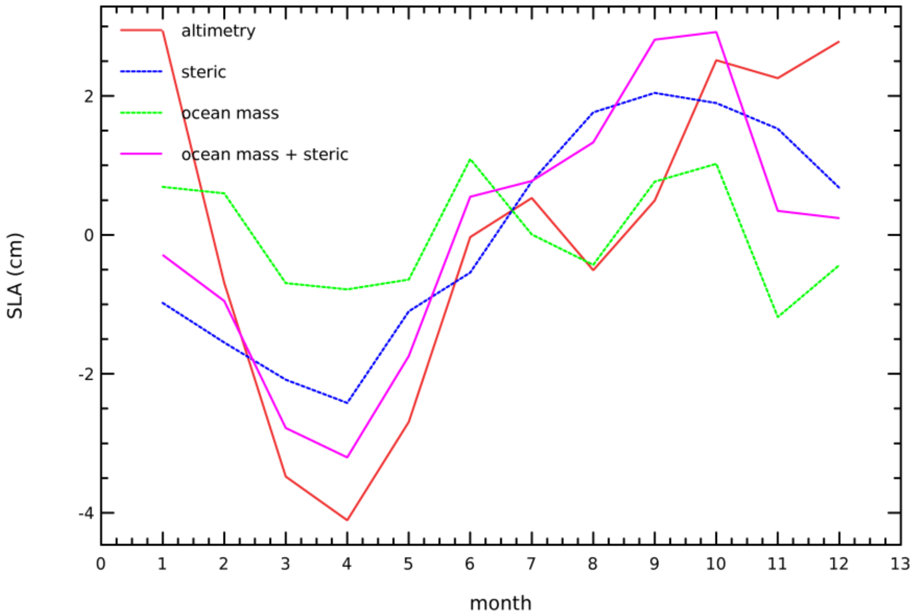

Fig. 5. Sea level annual cycle from altimetry (red), steric (blue), ocean mass (green) and the sum of steric and ocean mass components (violet).

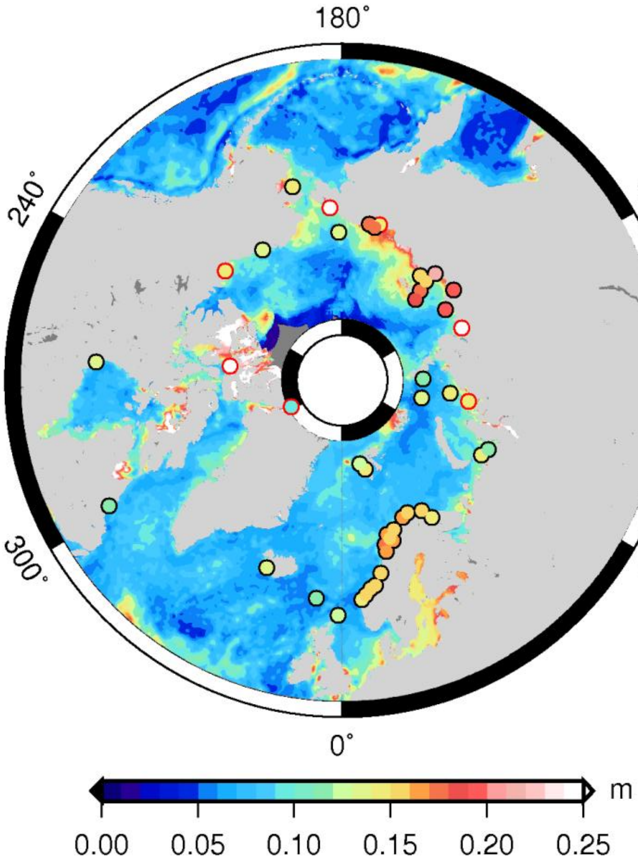

Fig. 6. Map of satellite altimetry SLA RMS values. The tide gauges SLA RMS are overlaid at the tide gauges positions.

OSD
9, 2375–2401, 2012

Title Page
Abstract Introduction
Conclusions References
Tables Figures
◂ ▸
Back Close
Full Screen / Esc
Printer-friendly Version
Interactive Discussion

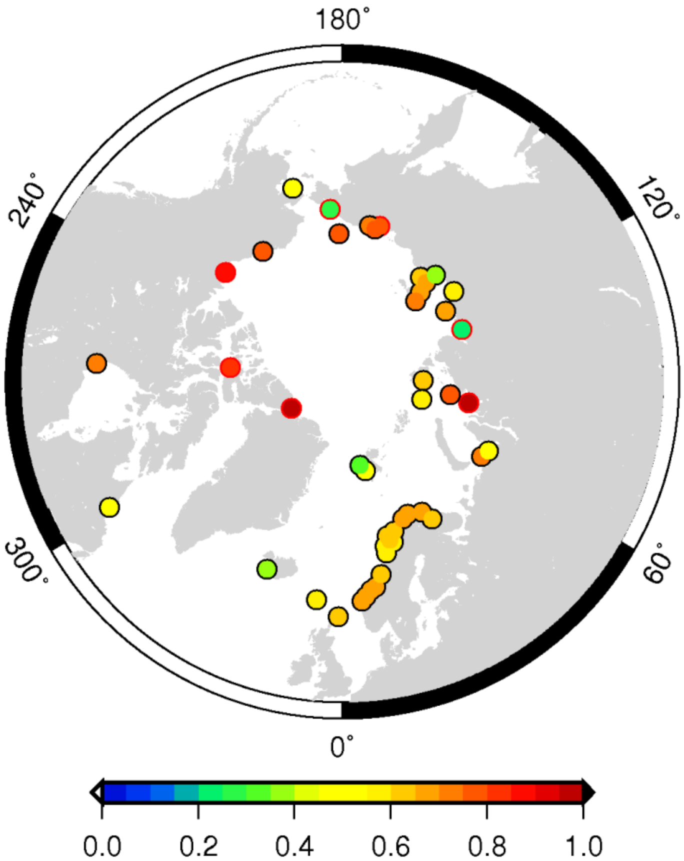

Fig. 7. Map the of the correlations coefficients between altimetry and tide gauges SLA time series. Red circles represent the stations where the correlation coefficient is not significantly different from 0 at the 1 % level.

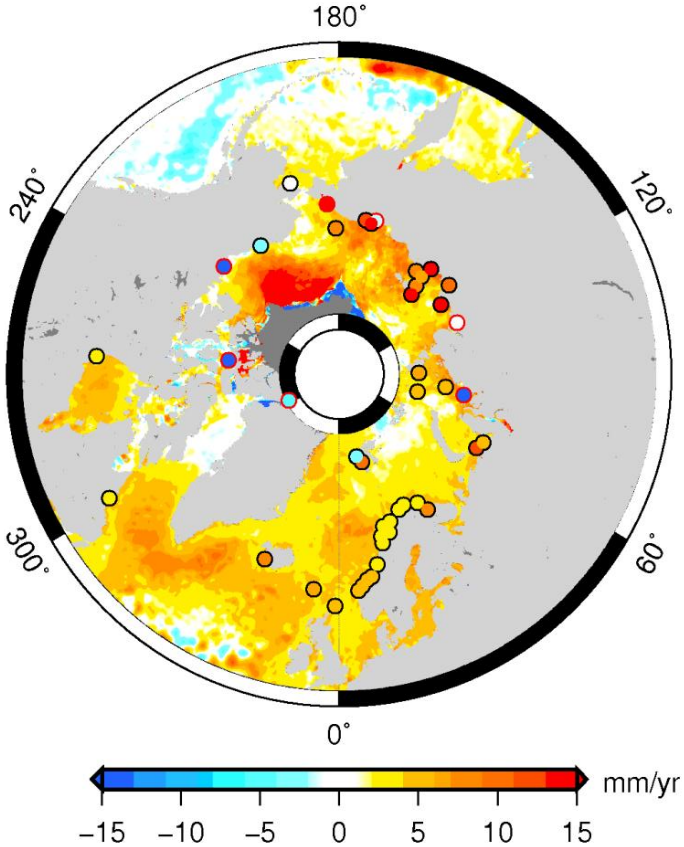

Fig. 8. Map of SLA trends from satellite altimetry over the 1993–2009 period. The tide gauges SLA trends are overlaid at the stations positions.

OSD
9, 2375–2401, 2012

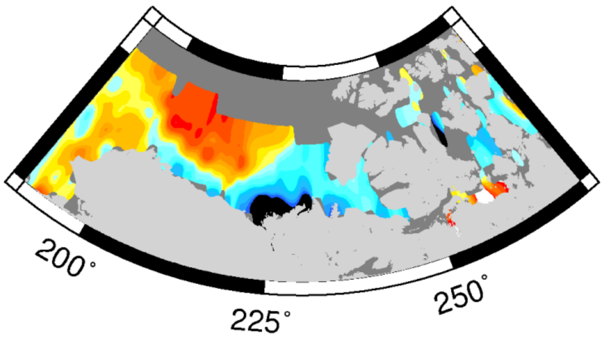

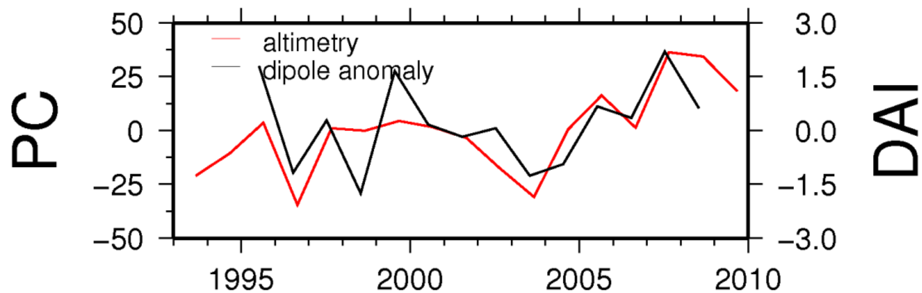

Fig. 9. (Top) map of the second mode of September mean altimetry SLA in the Beaufort Gyre area and (bottom) time series of the associated principal component in red, the Dipole Anomaly Index is overlaid in black.

OSD
9, 2375–2401, 2012

Sea level variability in the Arctic Ocean observed by satellite altimetry

P. Prandi et al.

Title Page
Abstract
Introduction
Conclusions
References
Tables
Figures
◀
▶
Back
Close
Full Screen / Esc
Printer-friendly Version
Interactive Discussion

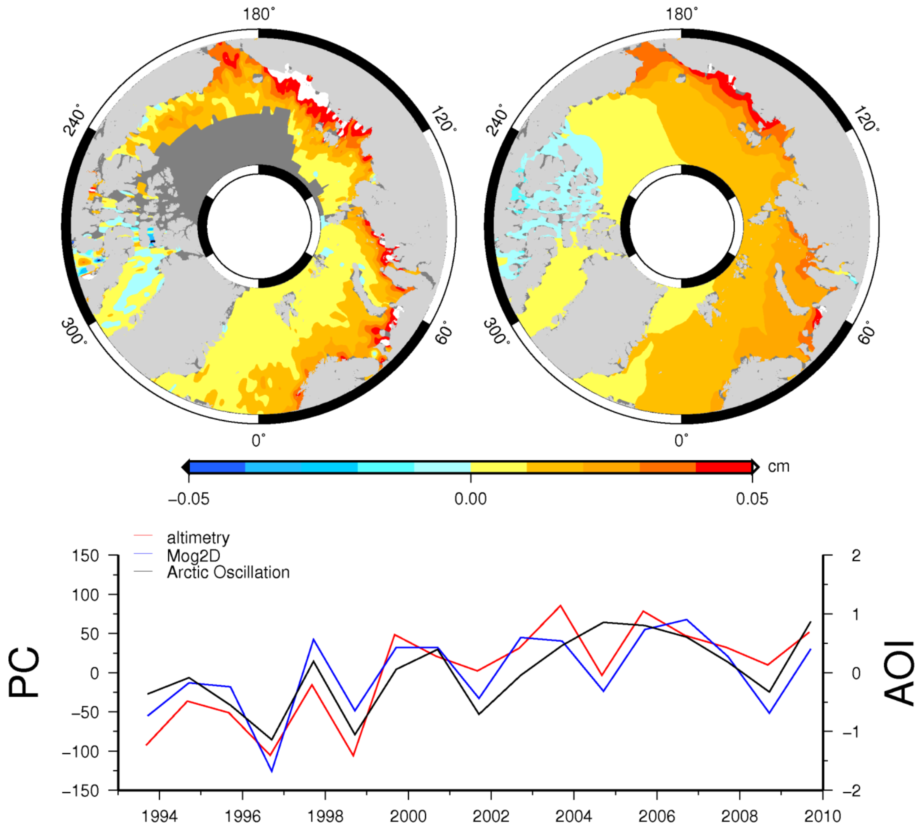

Fig. 10. (Top left) map of the first mode of September mean altimetry SLA, (top right) map of the first mode of September mean low-pass filtered DAC from Mog2d model and (bottom) time series of the associated principal components for altimetry in red and DAC in blue. The Arctic Oscillation Index is overlaid in black.

OSD
9, 2375–2401, 2012

Sea level variability in the Arctic Ocean observed by satellite altimetry

P. Prandi et al.